

Magnetic anisotropy, coupling, and transport in epitaxial Co/Cr superlattices on MgO(100) and (110) substrates

J. Johanna Picconatto and Michael J. Pechan
Department of Physics, Miami University, Oxford, Ohio 45056

Eric E. Fullerton
Materials Science Division, Argonne National Laboratory, Argonne, Illinois 60439

Superlattices of Co/Cr have been epitaxially sputtered onto MgO(100) and (110) substrates coated with epitaxial Cr(100) and (211) buffer layers. The Co thickness is fixed at 20 Å and the Cr thickness varied from 7 to 22 Å. On the MgO(110)/Cr(211) substrates, coherent hcp-Co(1100)/bcc-Cr(211) superlattice structures are formed. On MgO(100)/Cr(100), x-ray-diffraction results suggest strained hcp-Co(112̄)/bcc-Cr(100) superlattices. Magnetization measurements show fourfold magnetic in-plane anisotropy for the MgO(100) orientation and twofold for the MgO(110). By utilizing a simple model based upon perpendicular uniaxial anisotropies, we have concluded that the fourfold anisotropy has its origin in the second-order uniaxial Co anisotropy energy. The antiferromagnetic interlayer coupling strength exhibits a maximum value of 0.15 erg/cm² at a Cr thickness of 13 Å in the MgO(110) orientation. The MgO(100) orientation exhibits its strongest coupling of 0.55 erg/cm³ at 10 Å Cr thickness. Modest giant magnetoresistance values no larger than 3% are observed and we find no evidence of enhanced anisotropic magnetoresistance effects recently reported for Co(1100)/Cr(211) superlattices. © 1997 American Institute of Physics. [S0021-8979(97)49508-7]

I. INTRODUCTION

Co/Cr alloys and superlattices have long been the subject of study as candidates for increasing information density in recording media. This is in part due to the uniaxial crystal-line anisotropy inherent in hcp Co which gives it fundamentally unique magnetic properties in comparison with cubic Fe and Ni. Recently, investigators¹⁻⁴ have utilized epitaxial growth techniques to deposit coherent hcp Co layers with in-plane *c*-axis orientation. By choosing appropriate substrate and buffer layer crystalline orientations, one can control the symmetry of the in-plane magnetic anisotropy and the interlayer coupling strength (and therefore the magnetoresistance) in Co-based superlattices. Of particular technological interest are the small Co domains arising from perpendicular *c* axes oriented in registry with a fourfold symmetric substrate lattice. We have prepared epitaxial Co/Cr superlattices on MgO substrates for the purpose of investigating the anisotropy, coupling energies, and magnetotransport properties. Particularly noteworthy is our conclusion that both the direction and magnitude of the magnetic anisotropy associated with the fourfold symmetry samples can be understood as arising from the second-order Co uniaxial anisotropy energy.

II. EXPERIMENTAL DETAILS

Two series of [Co(20 Å)/Cr(*t*_{Cr})]₂₀ superlattices with (7 ≤ *t*_{Cr} ≤ 22 Å) were epitaxially sputtered onto single-crystal MgO(100) and (110) substrates. The substrates were mounted side by side onto the sample holder and simultaneously deposited. A 100 Å Cr layer was initially deposited at a substrate temperature of 600 °C resulting in epitaxial Cr(211) and (100) buffer layers on MgO(110) and (100), respectively.⁵ The substrate was then cooled to 150 °C and the samples were grown by sequential deposition of the Co

and Cr layers. This growth procedure has been successfully used to grow Fe/Cr and Co/Cr superlattices.^{2,5} On the MgO(110)/Cr(211) substrates, coherent hcp-Co(1100)/bcc-Cr(211) superlattices are formed, with x-ray diffraction, similar to those of Ref. 4. The in-plane epitaxial relationship is MgO[001]||Cr[011]||Co[0001]. On MgO(100)/Cr(100) substrates, the expected Co structure depends upon the Co layer thickness.³ For thick layers, the films are epitaxial hcp-Co(112̄) which grow with a bicrystal microstructure.⁶ The in-plane twin directions are MgO[001]||Cr[011]||Co[0001] and MgO[001]||Cr[011̄]||Co[0001]. For thinner layers the Co strains toward a bcc (100) layer. The x-ray-diffraction data of the present samples are similar to those reported in Ref. 2 suggesting strained hcp-Co(112̄) layers.

III. RESULTS AND DISCUSSION

Magnetic hysteresis measurements were performed using a vibrating sample magnetometer (VSM) at room temperature with the field in plane. Magnetotransport properties were measured from room temperature to 5 K using a standard four-terminal dc technique with a constant current and *H* in plane. To characterize the magnetic anisotropy we measured the remnant magnetization (normalized to the saturation magnetization) as a function of the azimuthal angle of the applied field. The results are shown in Fig. 1 for ferromagnetically coupled superlattices from each series. The remnant magnetization for the Co(1100) layers reflect the expected twofold uniaxial anisotropy with the easy axis along the MgO(001) direction. The Co(112̄) layers show a fourfold anisotropy with the easy axis along the MgO[011] and [011̄] directions. This high degree of in-plane anisotropy confirms the epitaxial nature of the layers. The strong fourfold anisotropy observed for the (100) samples is due to the twinned uniaxial microstructure. If we assume that the anisotropies from the twinned region are added (a reasonable

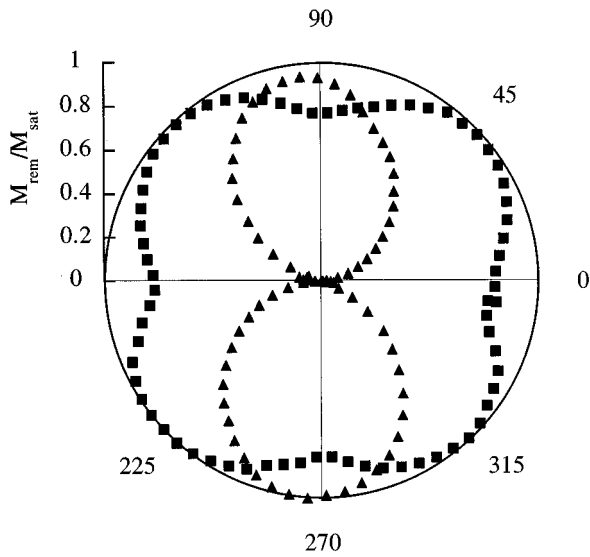


FIG. 1. Polar plot of the normalized remnant magnetization vs azimuthal (in-plane) angle for ferromagnetically coupled Co layer samples. Co/Cr(20 Å) grown on MgO(100) exhibits fourfold symmetry (squares) whereas Co/Cr(16 Å) on MgO(110) exhibits twofold symmetry (triangles).

assumption if the crystalline domains are small and exchange coupled) then the effective anisotropy energy equals

$$E = K_1 \sin^2 \theta + K_2 \sin^4 \theta + K_1 \cos^2 \theta + K_2 \cos^4 \theta$$

$$= K_1 + \frac{1}{2} K_2 (1 + \cos^2 2\theta), \quad (1)$$

where K_1 and K_2 are the first- and second-order uniaxial anisotropy constants and θ is the angle of the magnetization with respect to the MgO[001] direction. Therefore, we expect an effective cubic anisotropy with MgO[011] and [011] easy axis directions and strength determined by the second-order uniaxial anisotropy constant.

Magnetic hysteresis loops and giant magnetoresistance (GMR) curves measured with the applied field along the easy and hard axis for samples with the strongest antiferromagnetic (AF) coupling strength in each series are shown in Figs. 2 and 3, respectively. We first focus on the superlattices on MgO(110). The strongest AF coupling is observed for Cr layer thickness of 13 Å. The shape of the loop is characteristic of AF-coupled superlattices with strong uniaxial in-plane anisotropy⁷ as seen previously in Fe/Cr(211) and CoFe/Cu(110) superlattices on MgO(110).^{5,8} For the applied fields parallel to the easy axis, the system undergoes a metamagnetic transition from an antiparallel to parallel configuration at a switching field given by $H_s = 2J_1/M_s t_{Co}$, where J_1 is the bilinear interlayer coupling, and M_s is the saturation magnetization of the Co layer. Commensurate with the transition in the magnetization is a transition in the MR. Using the center of the offset hysteresis loops as an estimate of H_s (930 G), the interlayer coupling equals $J_1 = 0.13$ erg/cm². The coupling strength is considerably weaker in this Co(hcp)/Cr(bcc) system than in epitaxial Fe(bcc)/Cr(bcc) systems, which may result from the reduced symmetry of the bilayer structure and the resulting decrease in electron wave-

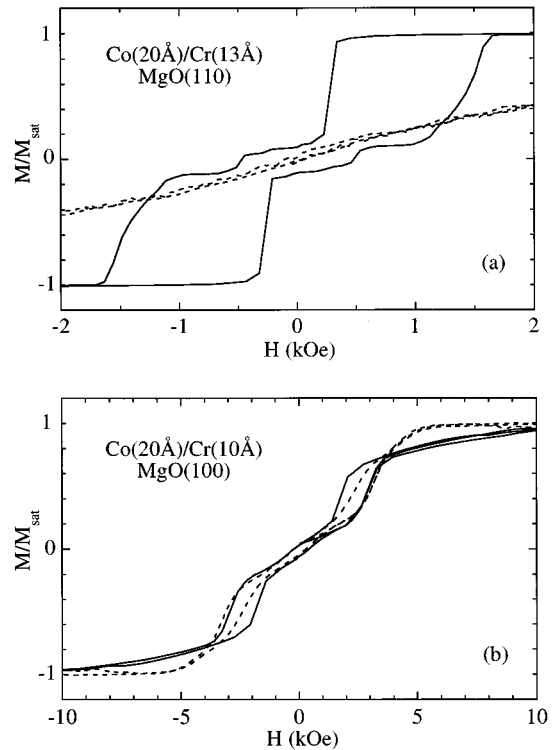


FIG. 2. Magnetic hysteresis loops for samples with peak AF-coupled Co layers: (a) Co/Cr(13 Å) on MgO(110) orientation and (b) Co/Cr(10 Å) MgO(100) orientation. Solid and dashed lines are data in the easy and hard in-plane directions, respectively. The top plot has been expanded to show easy axis details, but along the hard axis one observes the magnetization reach saturation at a field of approximately 8 kOe.

function overlap. When H is applied perpendicular to the easy axis, the Co layers coherently rotate to saturation at a field

$$H_s = (4J_1 + 8J_2 + 2t_{Co}K_1 + 4t_{Co}K_2)/M_s t_{Co},$$

where J_2 is the biquadratic interlayer coupling.⁹

For the superlattices on MgO(100), the strongest AF coupling was observed for $t_{Co} = 10$ Å in agreement with Ref. 2. The magnetization and MR show the expected dependence on the in-plane direction of the applied field [see especially Figs. 8(a) and 9(a) in Ref. 7]. The saturation fields for the applied field parallel to the easy and hard axes are 4.7 and 11.3 kOe, respectively. The difference in saturation fields reflects the fourfold anisotropy. Assuming a fourfold anisotropy described by Eq. (1), the expected saturation fields are $H_s \approx (4J_1 + 8J_2 \pm 2K_2)/M_s t_{Co}$ where the + and - correspond to the hard and easy axes, respectively. From the difference in the H_s values, the estimated value for K_2 is 2.3×10^6 ergs/cm³, which is comparable to the room-temperature value of K_2 for bulk Co, 1.5×10^6 ergs/cm³. This suggests that the fourfold anisotropy results from the uniaxial structures oriented perpendicularly within a layer rather than intrinsic anisotropies arising from a coherent bcc crystal structure. The value of the exchange coupling, determined from the average saturation field, is $J_1 + 2J_2 = 0.55$ erg/cm².

The GMR values are generally quite small in comparison to Fe/Cr superlattices, room-temperature values of 0.8%

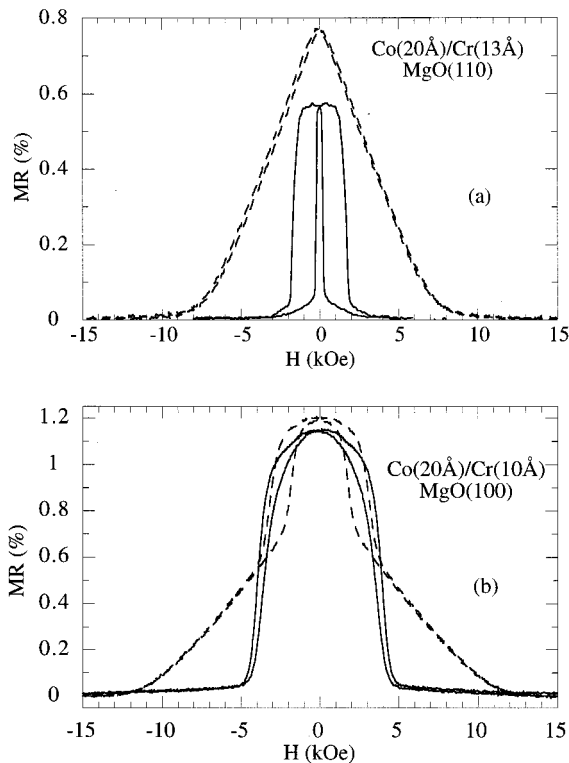


FIG. 3. In-plane magnetoresistance data for samples shown in Fig. 2: (a) Co/Cr(13 Å) on MgO(110) and (b) Co/Cr(10 Å) on MgO(100). Dashed (solid) lines represent data taken with the field in the hard (easy) in-plane direction.

and 1.2% for the AF-coupled superlattices on MgO(110) and (100), respectively, increasing to 2.0% and 3.2% at 5 K. The results are only weakly dependent on the relative direction of the current with respect to the field and crystallographic axis, characteristic of the anisotropic MR of Co. We did not observe the large transverse MR reported for Co(1100)/Cr(211) superlattices.⁴ For H along the Co[1120] and the current par-

allel to the Co[0001], the authors report MR ratios up to 18%. For other orientations of the applied field and current, MR values <1% were reported.

Modeling of both the magnetization and the MR data is underway using approaches described in Refs. 7 and 9. In addition, torque measurements are planned to better isolate anisotropy from coupling effects and to provide a more insight into the relationship between K_1 and K_2 in each of the MgO(110) and (100) series. A key question underlying the magnetic behavior of these systems is the role played by micromagnetics. In other words, to what extent is the assumption [leading to Eq. (1)] of small bicrystalline domains with strong interdomain exchange valid in our system? Micromagnetic modeling, such as that successfully employed recently by Peng *et al.*,¹⁰ may help in addressing such questions.

ACKNOWLEDGMENTS

We wish to thank Zachary Hilt for taking the data for Fig. 1 and C. H. Sowers for sample preparation. This work was supported by U.S. Department of Energy, Basic Energy Sciences—Materials Sciences, under Contracts No. W-31-109-ENG-38 (ANL) and No. DE-FG02-86ER45281 (Miami).

- ¹F. Schreiber, Z. Frait, Th. Zeidler, N. Metoki, W. Donner, H. Zabel, and J. Pelzl, *Phys. Rev. B* **51**, 2920 (1995).
- ²G. R. Harp and S. S. P. Parkin, *Appl. Phys. Lett.* **65**, 3063 (1994).
- ³N. Metoki, W. Donner, and H. Zabel, *Phys. Rev. B* **49**, 17 351 (1994).
- ⁴J. C. A. Huang, Y. Liou, Y. D. Yao, W. T. Yang, C. P. Chang, S. Y. Liao, and Y. M. Hu, *Phys. Rev. B* **52**, R13 110 (1995).
- ⁵E. E. Fullerton, M. J. Conover, J. E. Mattson, C. H. Sowers, and S. D. Bader, *Phys. Rev. B* **48**, 15 755 (1993).
- ⁶A. Nakamura and M. Futamoto, *J. Appl. Phys.* **32**, 1410 (1993).
- ⁷W. Folkerts, *J. Magn. Magn. Mater.* **94**, 302 (1991).
- ⁸K. Inomata and Y. Saito, *Appl. Phys. Lett.* **61**, 726 (1992).
- ⁹M. Grimsditch, S. Kumar, and E. E. Fullerton, *Phys. Rev. B* **54**, 3385 (1996).
- ¹⁰Q. Peng, H. Neal Bertram, Nina Fussing, Mary Doerner, Mohammad Mirsamaanj, David Margulies, Robert Sinclair, and Steven Lambert, *IEEE Trans. Magn.* **MAG-31**, 2821 (1995).